An Adaptive Data-driven Method Based on Fuzzy Logic for Determining Power System Voltage Status

Sirwan Shazdeh, Hêmin Golpîra, *Senior Member*, *IEEE*, and Hassan Bevrani, *Fellow*, *IEEE*

***Abstract*—This paper proposes an adaptive method based on fuzzy logic that utilizes data from phasor measurement units (PMUs) to assess and classify generating-side voltage trajectories. The voltage variable and its associated derivatives are used as the input variables of a fuzzy-logic block. In addition, the voltage trajectory is compared with the pre-selected pilot-bus voltage to make a reliable decision about the voltage operational state. Different types of short-term voltage dynamics are considered in the proposed method. The fuzzy membership functions are determined using a systematic method that considers the current situation of the voltage trajectory. Finally, the voltage status is categorized into four classes to determine appropriate remedial actions. The proposed method is validated on a IEEE 73-bus power system in a MATLAB environment.**

***Index Terms*—Fuzzy logic, fault-induced delayed voltage recovery, phasor measurement unit (PMU), short-term voltage stability, situational awareness, voltage classification.**

I. Introduction

DUE to the fast-growing complexity of power systems, whether from a software or hardware perspective, the steady-state operation of power systems is often exposed to different disturbances. In addition, modern power systems are heavily loaded close to their capacity limits due to economic and environmental issues. The increasing penetration of flexible electrical loads into power systems also makes power system dynamics more complex than before. Consequently, the stable operation of power systems is frequently threatened by their low-stability margins. Under these circumstances, the voltage stability (VS) encounters significant challenges. Therefore, it is necessary to have proper knowledge of the VS before entering into an unacceptable operation area. This in turn allows the system operator (SO) to maintain system stability and restore the voltage profile without significant load shedding or generator disconnection.

VS is defined as "the ability of a power system to maintain steady-state voltages close to the nominal value at all buses in the system after being subjected to a disturbance [1]." VS issues may trigger protection schemes in power systems, which in turn may result in cascading outages.

Among many VS issues, short-term voltage instability (STVI), fault-induced delayed voltage recovery (FIDVR), and fast voltage collapse are the most harmful phenomena that result from the penetration of fast load dynamics in modern power systems. These phenomena are inherently fast, making their evaluation challenging. STVI is defined as the inability of a power system to deliver the required reactive power due to the fast interaction of the load components when the voltage is at a low level. By contrast, FIDVR refers to the slow recovery of voltage following fault clearance under low-voltage conditions. However, a voltage collapse indicates a significant decrease in voltage in a noticeable area of the power system following a disturbance [2]. Various efforts have been made based on different concerns to assess the VS of power systems [3], as discussed in the following subsections.

Notably, despite the efficacy of the existing methods in identifying these phenomena, most of them consider only one of the mentioned phenomena. In addition, they make decisions about the voltage status only when they exceed a predefined secure area. Although these principles may lead to accurate identification, they result in expensive remedial actions for only single case of the aforementioned phenomena. Furthermore, the existing methods do not allow for preemptive measures to be taken in a timely manner, as they only identify the issue after they exceeded a predefined area. This often requires the SO to perform severe and costly remedial actions to maintain power system security. Therefore, this paper proposes a new type of voltage classification that enables low-cost preemptive actions to be taken before potential threats increase.

In general, VS assessment methods can be categorized into event-based [4] and response-based methods. Because event-based methods rely on the type of disturbance, these methods are unreliable given the complexity of modern power systems. Due to the uncertainties in loads and generation units, the challenges in terms of the reliability and compre-

Manuscript received: May 18, 2023; revised: August 5, 2023; accepted: September 20, 2023. Date of CrossCheck: September 20, 2023. Date of online publication: December 5, 2023.

This work was supported in part by Smart/Micro Grids Research Center (SMGRC), University of Kurdistan.

S. Shazdeh and H. Bevrani (corresponding author) are with the SMGRC, University of Kurdistan, Sanandaj, Iran (e-mail: s.shazdeh@uok.ac.ir; bevrani@uok.ac.ir).

H. Golpîra is with Power Systems Modeling & Simulation Lab, Department of Electrical Engineering, University of Kurdistan, Kurdistan, Sanandaj 66177-15175, Iran (e-mail: hemin.golpira@uok.ac.ir).

DOI: 10.35833/MPCE.2023.000325

hensibility of event-based methods have led to increased focus on response-based methods. Response-based methods comprise two classes: model-based and data-driven methods.

1) Model-based Methods

Traditionally, VS is accomplished by power system models. To achieve specific aims, model-based methods require solving relevant sophisticated differential equations using time-domain simulations. Among these methods, *P-V* and *Q-V* curves for specified load buses are the most conventional schemes, requiring enormous power flow calculations [5]. Thus, these methods have a high-computational burden and complicated procedures, which pose speed and simplicity challenges. Probabilistic analytical methods utilize power system models [6] to provide appropriate responses based on specific voltage situations. However, the effects of uncertainties on the accuracy of probabilistic methods and their excessive computations present considerable disadvantages. These challenges have prompted the development of data-driven methods.

2) Data-driven Methods

To address the aforementioned drawbacks and considering the major progress in communication infrastructure and wide-area measurement systems (WAMSs), data-driven methods have recently gained attention because of their high speed and accuracy in VS assessments. In general, data-driven methods for VS assessment involve machine-learning and analytical-measurement methods.

1) Machine-learning methods

Machine-learning methods such as artificial neural networks [7], decision tree [8], and space vector machines [9] are efficient methods for addressing problems related to extensive information analysis, extraction of valuable features [10], and classification of voltage states [8]. Notable efforts have been made using machine-learning methods to assess voltage states with a focus on speed, accuracy, and simplicity [8]. However, despite the growing interest in machine-learning methods, they face substantial challenges such as excessive data-based training, adaptability issues with power system development, parameter tuning, and mismatched data that contribute to the training process with realistic power system data [9].

2) Analytical-measurement methods

Unlike machine-learning methods, analytical-measurement methods have been developed to derive cognitive indices based on the mathematical equations that govern the phenomena under study. These methods simplify the decision-making process compared with model-based methods [11]. Various VS indices have been proposed in this category. For example, the transient voltage severity index (TVSI) is examined in [12] to assess voltage violations. However, despite the dependency of this index on data for decision-making, the TVSI is often inaccurate under oscillatory and FIDVR conditions. Furthermore, determining the threshold is difficult because of conflicts with normal conditions during the FIDVR situation.

In another attempt, the trajectory violation index (TVI), which is a model-free assessment index, is introduced in [13] to assess VS, where the derivation of the index relies on the exponential threshold, which is case-dependent. In addition, the VS risk index (VSRI), which relies on moving-averaged and normalized voltage deviations, is examined in [14] for long- and short-term VS evaluations. Although the index uses a moving-average window in the decision-making process, the assessment method cannot differentiate between voltage problems such as FIDVR and oscillatory situations. However, in [15], the voltage recovery index is improved based on the probability density function and self-impedance of buses to determine short-term voltage stability (STVS) status.

In the area of analytical-measurement VS assessment, some studies have examined the methods based on the Thevenin equivalent circuit. The voltage instability predictor is a well-known index that relies on the Thevenin impedance compatibility with the load impedance. This method attempts to determine the maximum load power by comparing the equivalent Thevenin impedance with the load impedance. Although this index is used for long-term voltage instability assessment, it is used in [16] for short-term purposes. In a complementary effort [17], the effects of the generator var restrictions are considered when obtaining Thevenin equivalent parameters. Reference [18] proposes a Thevenin-parameter-based index to trigger the required remedial action with respect to the voltage status. Obtaining the equivalent Thevenin impedance is challenging and has become even more critical for newly emerging flexible loads.

In [19], voltage and recovery time deviations are introduced as two key factors for assessing voltage situations following fault clearance. These factors are utilized by a fuzzy-logic controller to determine the voltage condition and perform an undervoltage load-shedding scheme, if required. In another study [20], the rate of change of voltage (RoCoV) recovery and recovery time estimation are used to determine the FIDVR status of the generator bus and trigger under-voltage load shedding. However, these methods rely only on instantaneous voltage deviations in making decisions, which may affect the detection accuracy. As another limitation, these methods cannot simultaneously consider the FIDVR, STVI, and oscillatory conditions.

Most existing methods focus only on voltage assessment when the voltage is outside a predefined area. This in turn requires numerous corrective actions to address complex situations. In addition, these methods often lack appropriate thresholds, necessitating complex studies to improve the assessment accuracy. This issue is discussed further in the comparison section of this paper.

To address these drawbacks, this paper proposes a fuzzy-logic-based framework to identify the voltage status and classify the voltage condition into the four classes of steady state, alarm, emergency, and high risk. Some existing studies that perform VS assessments, in which the present voltage value is compared with its previous behavior within a specific window, may fail in proper decision making. Hence, the bus voltage is compared with the reference pilot bus voltage to provide a comprehensive perspective based on a strict bus in the proposed method. In addition, the results of the implementation of the proposed method in this paper are involved

in the decision-making process.

Although the FIDVR, STVI, and oscillatory conditions are considered in the assessment process, they are independently investigated in previous studies. Notably, unlike some existing methods, the voltage status assessment is performed when the voltage trajectory remains within the allowable range of the North American Electric Reliability Council (NERC) criteria [21] as a free-model and free-threshold algorithm. This method can provide pre-awareness of the voltage status as a voltage robustness indicator for preemptive and less costly actions and a classification of generator buses. The voltage magnitude, RoCoV, RoCoV based on the pilot bus ($RoCoV_p$), and time duration, are used as inputs for the fuzzy-logic scheme to classify the voltage status.

The contributions of the paper are as follows.

1) A simple data-driven fuzzy-logic method is proposed to determine the voltage status.

2) The voltage situation is classified into four categories when it lies within the allowable area introduced by the NERC to implement proper measures against the circumstances created.

3) The effects of the FIDVR, STVI, and oscillatory conditions are simultaneously considered in the classification process.

4) The developed assessment process considers the behavior of the non-pilot bus voltage based on the pilot bus.

5) The history of the voltage trajectory is involved in each averaging window, which improves decision making in terms of broad data samples.

The remainder of this paper is organized as follows. Section II provides the proposed methodology. The developed fuzzy-logic method is explained in Section III. Simulation results are assessed in Section IV to confirm the efficacy of the proposed method. Finally, the overall features of the results are summarized in Section V.

II. Proposed Methodology

Determining the power system voltage status results in proper situational awareness and provides conditions for conducting appropriate corrective and preventive actions. However, maintaining the generating units in an operational state is essential to effectively satisfy the reactive power requirements of the system. Hence, the status of the voltage situation is investigated based on PV bus voltage trajectories in this paper. To this end, the following hypotheses are first considered to simplify the voltage assessment process.

A. Hypotheses

1) The NERC relevant to voltage ride-through in [21] is used as a general framework in several steps. This criterion was proposed by the NERC to keep generators in service during voltage excursions. Therefore, it serves as a supportive framework for the proposed method in this paper. In addition, the oscillatory effects of the voltage are considered based on the Western Electricity Coordinating Council (WECC) criteria for transient voltage [22]. According to the conservative nature of the NERC criterion, the proposed method for voltage-status classification is applied only when the voltage trajectory remains within the allowable area, as defined in Fig. 1 [21], where t_c denotes the instant of fault clearance. However, the NERC criterion considers only the upper and lower voltage limits. Therefore, it may be useful to include more information about the voltage trajectory within these limits. Despite satisfying the criterion for voltage recovery after fault clearance, the voltage may track an abnormal trend due to load dynamics, resulting in STVI. The NERC specifies that generators must be able to withstand different voltage levels for various durations, particularly during under-voltage situations. For upper-voltage considerations, the voltage level must remain below 1.1 p.u. at all times.

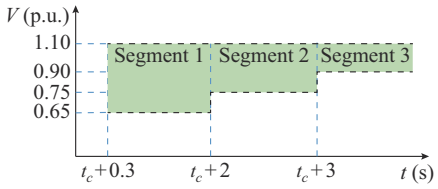

Fig. 1. Modified voltage ride-through criterion based on NERC.

2) The voltage magnitude trajectory may exhibit an oscillatory feature due to transient conditions following a severe disturbance. Thus, it can have a destructive effect on fuzzy-logic classification. To alleviate this effect, the averaged voltage in a window length involving 20 samples and taking 0.33 s is used in the fuzzy logic. This measure can reduce the oscillatory effect of a voltage signal with frequency oscillations greater than 3 Hz. This helps remove oscillations with frequencies higher than 3 Hz. This strategy indicates the overall voltage position during the 0.33 s concerning measurement errors and the oscillatory voltages with high frequency during the decision-making process. The averaging-related window length consists of five past samples accompanied by 15 updated samples. The instant of the obtained average value belongs to the latest received corresponding time.

3) The pilot bus in an area is known as the firmest bus in that area. Various criteria can be used to select a pilot bus such as the conventional maximum short-circuit current [23]. In this paper, the pilot bus in each area is connected to a PV bus with a high short-circuit current. This pilot bus is more robust against oscillations than the others and thus can provide a reliable decision reference for the situation. This is unlike some methods that compare the voltage with their historical trend. It is noteworthy that in addition to a comparison with the pilot bus, the properties of individual buses such as RoCoV, voltage magnitude behavior, and time duration are also used to provide a comprehensive assessment of the voltage status. Moreover, comparing the voltage trajectory with that of other buses (except for the pilot bus) can result in an unreliable decision because of undesirable behavior and confusing results. Although several methods are used for selecting a pilot bus, this paper considers a conventional method to assess the VS. Thus, the voltage behavior of non-pilot buses is evaluated based on the pilot bus voltage. In addition, the pilot bus is assumed to be pre-selected.

B. Overall Framework

Figure 2 illustrates the overall process of the proposed method for assessing the voltage status, where $|V_{bus}|_i$ is the voltage of bus i. The input definition block is next explained in detail, and the fuzzy-logic block is addressed in Section III.

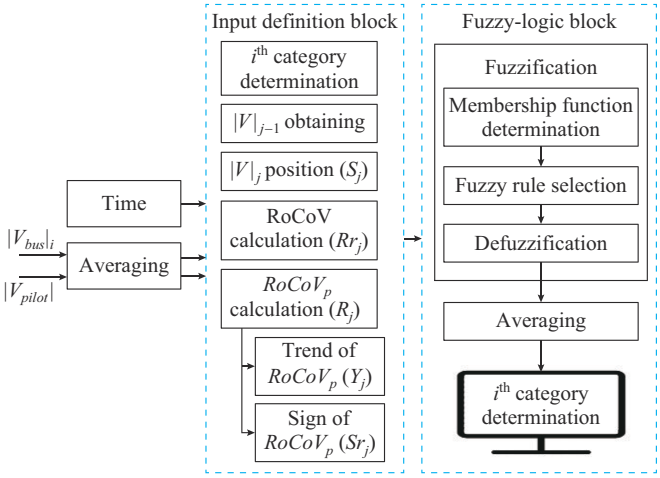

Fig. 2. Overall process of proposed method for assessing voltage status.

Voltage assessment is conducted in three segments, as shown in Fig. 1, over time. During normal operation, the voltage trajectory is expected to approach steady-state conditions over time. In this paper, the fuzzy-logic block considers seven variables for decision making. These variables include the slope of voltage magnitude with respect to the lower voltage at that segment, the previous sample of voltage magnitude ($|V|_{j-1}$), the $RoCoV_p$, the sign of the $RoCoV_p$, the trend variations of $RoCoV_p$ compared with its previous value, the RoCoV with respect to its past sample, and the time. These variables are described as follows.

The desired voltage trajectory is achieved when it continuously approaches its nominal value. Therefore, the slope of the present voltage magnitude sample with respect to the lower-voltage bound at the previous sample time provides useful information regarding its distance to the lower-voltage bound and its trend toward the normal state. Thus, the slope of the voltage magnitude is included as an input variable in the fuzzy-logic block to obtain better classification results. This input variable is defined based on (1).

$$S_j = \frac{|V|_j - |V_{base}|^i}{t^j - t^{j-1}} \tag{1}$$

where $|V_{base}|^i$ is the lower voltage at the i^{th} segment; $|V|_j$ is the current variable sample of the non-pilot bus voltage magnitude; and j is the current variable sample. The time variable is considered as the second input to the fuzzy-logic block. This input variable provides information on the variations in the voltage trajectory.

However, assessing the voltage status of the generator buses based on the pilot bus, which is the strongest of the other buses in the area, improves comprehensive situational awareness. The pilot bus provides more reliable countermeasures for the reactive power demand and better response compared with other buses in the area [23]. Therefore, the voltage profile of the pilot bus is more informative than those of the other buses. Thus, assessing the voltage behavior of non-pilot buses based on that of pilot buses is recommended. It is noteworthy that a pilot bus is pre-selected in this paper. Therefore, the $RoCoV_p$ and its profile are used in the fuzzy-logic method to investigate the non-pilot bus voltages based on the pilot bus. The $RoCoV_p$ is defined based on (2).

$$R_j = \frac{|V|_j - |V_{pilot}|_{j-1}}{t^j - t^{j-1}} \tag{2}$$

where $|V_{pilot}|_{j-1}$ is the voltage magnitude of the pilot bus at the previous sample time. The behavior of the $RoCoV_p$ is determined by its directional specifications. In addition, the variations in its magnitude are determined based on its previous value. Therefore, the ratio of the absolute value of the obtained $RoCoV_p$ at the present sample time to its value in the past sample indicates the magnitude variations, as expressed in (3).

$$Y_j = \frac{|R_j|}{R_{j-1}} \tag{3}$$

Furthermore, the negative or positive signs of $RoCoV_p$ at the present instant indicates the direction of the obtained slope, providing additional information for better decision making as the fourth input.

$$Sr_j = Sign(R_j) \tag{4}$$

The voltage magnitude at the previous sample time provides reliable information for the fuzzy-logic method to generate accurate results. This information assists in properly considering the effects of oscillatory trends on the voltage profile.

As the final input, the RoCoV, based on its previous voltage magnitude, elucidates the trend of the voltage profile between two consecutive samples. Combining it with other inputs completes the classification. The RoCoV function is derived based on (5).

$$Rr_j = \frac{|V|_j - |V|_{j-1}}{t^j - t^{j-1}} \tag{5}$$

III. Developed Fuzzy-logic Method

Figure 3 shows the overall structure of the fuzzy-logic method. The first process involves eight membership functions for fuzzification. Typically, the input and output variables are subjected to simple triangular or trapezoidal membership functions. Figure 3 provides an overview of the membership functions (MFi) for the input and output variables. The membership function parameters for some of the input variables are adaptively changed based on the current segment and the variables involved in the classification. The subsequent subsections elaborate on the details of each membership function.

A. Membership Function Design

Accordingly, MF1, which is the membership function block associated with the voltage magnitude position, consists of three trapezoidal membership functions within its specified range.

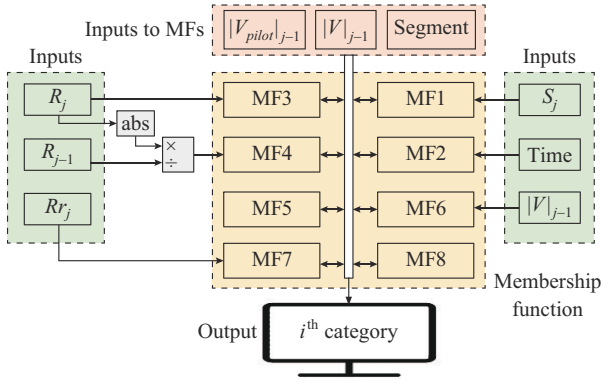

Fig. 3. Overall structure of fuzzy-logic method.

This membership function determines the area of the voltage magnitude position by considering its slope from the lower-bound value of the previous sample time. The lower bound of the voltage magnitude varies depending on the current segment. For Segments 1-3, this value is set to be 0.65, 0.75, and 1 p.u., respectively. The defined parts of MF1 are categorized into three linguistic values: L (low), M (medium), and H (high). Figure 4 illustrates the process for determining the parameters of MF1, where subscripts u and l denote the upper and lower bounds, respectively; and $|V|_{up}$ is the upper bound of the higher area for segments 1-3.

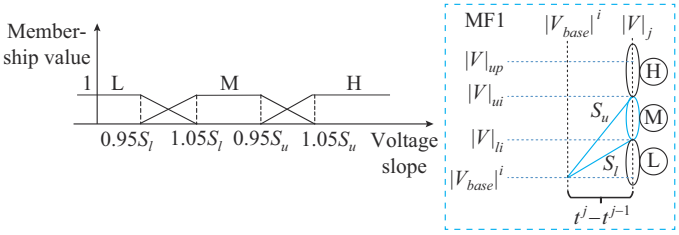

Fig. 4. Process for determining parameters of MF1.

Notably, the values associated with $|V|_{ui}$ and $|V|_{li}$ vary depending on the current segment. $|V|_{ui}$ values for all segments are set to be 1.05 p.u.. The values corresponding to $|V|_{li}$ are equal to 0.92, 0.95, and 0.975 p.u. in Segments 1-3, respectively.

MF2 is a part of the membership function block associated with the time-variable input. In general, in each segment, MF2 consists of two triangular membership functions. In Segment 1, the L_1 linguistic parameter is dedicated to the triangular membership function between $t_{01} = t_c + 0.3$ s and $t_{11} = t_c + 1.15$ s. The H_i parameters belong to the second triangular membership function from t_{11} to $t_{21} = t_c + 1.7$ s. In Segment 2, the two membership functions take t_{21} between $t_{12} = t_c + 2.2$ s and $t_{22} = t_c + 2.7$ s, respectively. The relevant time parameters in Segment 3 are equal to t_{22}, $t_{13} = t_c + 3.2$ s, and $t_{23} = t_c + 4.4$ s, respectively. Figure 5 illustrates the distribution principle of the membership functions for the time variable input, in which i refers to the understudy segment. The third membership function is associated with $RoCoV_p$, which is based on the voltage magnitude of the pilot bus at the previous sample time.

Figure 6 shows the membership function pertaining to $RoCoV_p$.

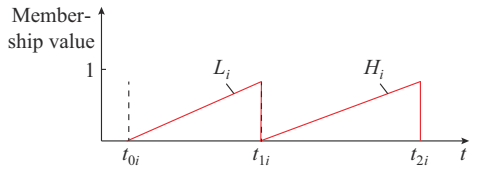

Fig. 5. Distribution principle of membership functions for time variable input.

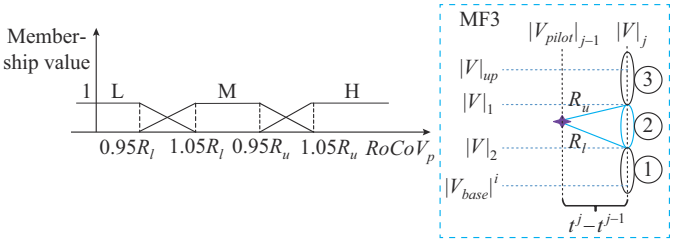

Fig. 6. Membership function pertaining to $RoCoV_p$.

In this case, R_{ui} denotes the upper bound of $RoCoV_p$, which can be determined using (6) and R_{li} as the lower bound is written as (7).

$$R_{ui} = \frac{|V|_1^i - |V_{pilot}|_{j-1}}{t^j - t^{j-1}} \tag{6}$$

$$R_{li} = \frac{|V|_2^i - |V_{pilot}|_{j-1}}{t^j - t^{j-1}} \tag{7}$$

The $|V|_1$ and $|V|_2$ are the voltage magnitude boundaries, and i refers to the understudy segment. The values for $|V|_1$ in Segments 1 and 2 and in the first part of Segment 3 are set to be 0.8, 0.9, and 0.95 p.u., respectively.

The values for V_2 in Segments 1 and 2 and the first part of Segment 3 are 1, 1.06, and 1.05 p.u., respectively. The upper and lower bounds in the second part of Segment 3 are set to be 1.02 and 0.975 p.u., respectively.

In addition, the variations in voltage magnitude of the pilot bus demonstrate the adaptive nature of the membership function status. As shown in Fig. 6, MF3, which is the membership function block associated with $ROCOV_p$, consists of three trapezoidal membership functions with designated ranges and linguistic parameters.

MF4 and MF5 are relevant for determining the $RoCoV_p$ trajectory. Accordingly, MF4 identifies the $RoCoV_p$ trend when it declines continuously in two consecutive samples. Thus, when the ratio of current absolute $RoCoV_p$ value to the $RoCoV_p$ value at the previous sample time is less than −1, it implies that the $RoCoV_p$ value has increased, whereas its previous sample has a negative value. MF4 includes two trapezoidal membership functions, as illustrated in Fig. 7.

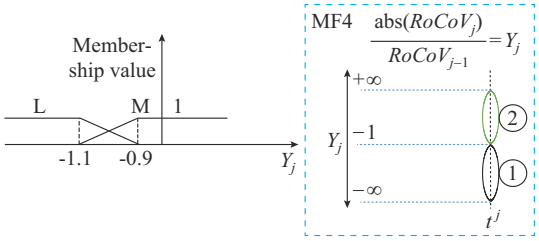

Fig. 7. Characteristics of MF4 as related to Y_j.

MF5 specifies the sign of the $RoCoV_p$ based on the membership functions, as shown in Fig. 8.

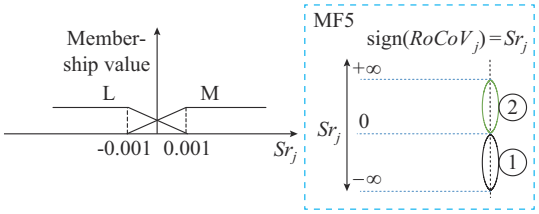

Fig. 8. Characteristics of MF5 as related to sign of $RoCoV_p$.

The remaining MFs refer to the behavior of the self-voltage magnitude. As previously mentioned, when the voltage trajectory remains less than 0.8 p.u. for a time duration more than 0.25 s, it indicates the potential high-risk circumstance for the voltage [22]. Thus, with respect to 0.33 s between two consecutive samples, the previous voltage magnitude value and RoCoV based on the past voltage magnitude value simplify the decision making for this situation. Accordingly, MF6, which is related to the past voltage magnitude variable, consists of three trapezoidal membership functions.

Figure 9 illustrates the characteristics of MF6, and the MF block is related to the previous voltage magnitude variables. $|V|_1$ and $|V|_2$ values are fixed at 0.8 and 1.05 p.u., in Segments 1 and 2, respectively. By contrast, these same variables in Segment 3 are set to be 0.95 and 1.05 p.u., respectively.

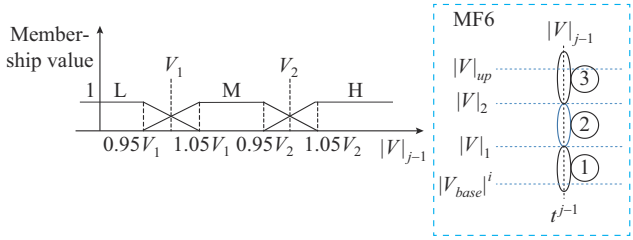

Fig. 9. Characteristics of MF6.

In addition, MF7, which is the membership function block associated with RoCoV, consists of three trapezoidal membership functions. As Fig. 10 shows, Rr_u and Rr_l slopes depend on $|V|_{2u}$, $|V|_{2l}$ and the previous voltage magnitude. $|V|_{2u}$ in Segments 1 and 2 is 0.8 p.u., whereas $|V|_{2l}$ is 0.9 p.u.. These same parameters in the first part of Segment 3 are 0.925 and 1.075 p.u., respectively. In addition, the space between the upper and lower bounds is limited to 0.95-1.06 p.u. in the second part of Segment 3.

Finally, MF8 refers to the output variable consisting of two trapezoidal and triangular membership functions.

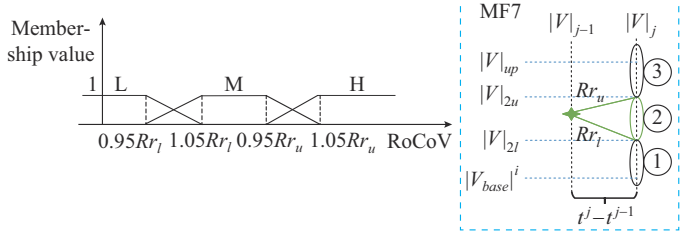

Fig. 10. Characteristics of MF7.

According to the combination of the input variable effects using the fuzzy-logic block, the output is categorized into four statuses: normal, alarm, emergency, and high risk. Figure 11 shows the characteristics of MF8, and the MF block is related to the output variable.

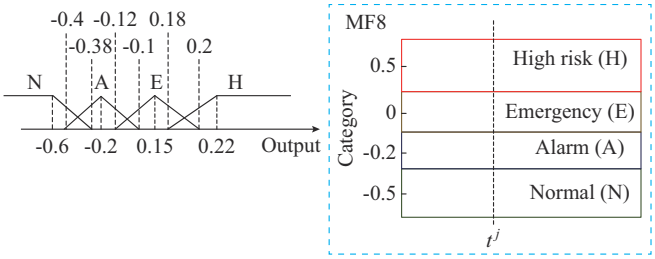

Fig. 11. Characteristics of MF8.

B. Determination of Fuzzy Rules

Based on the existing eight MFs and the numbers of their membership functions, defining extensive rules for the classification intention is then necessary. In general, 1944 rules use a combination of different membership functions. For clarification, the fuzzy rules related to each category output are described in detail.

These fuzzy rule bases are listed in Table I. These are interpreted as the states in which the voltage magnitude slope lies in the lower area in a similar manner as $RoCoV_p$, where the past sample of the voltage magnitude is less than 0.9 p.u. and RoCoV has a slope in area 1. Despite the negative sign of $RoCoV_p$ in the two previous consecutive samples, it showed a declining trend. The assessment is performed in Segment 3. This situation is declared as high risk by the fuzzy-logic method. Regarding the placement of the previous voltage magnitude sample at a value less than 0.9 p.u., the voltage trajectory follows an improper trend.

TABLE I
FUZZY RULE BASES

Row	MF1	MF2	MF3	MF4	MF5	MF6	MF7	MF8
1	L	L_3	L	L	L	L	L	H
2	H	H_2	H	H	H	M	H	E
3	M	L_3	M	H	H	L	M	A
4	M	L_3	M	H	H	M	M	N
5	L	H_3	L	L	L	M	L	H
6	L	H_2	L	L	L	L	L	H

The second row in Table I refers to a high-voltage threat following a fault clearance. In this case, the voltage magnitude slope, $RoCoV_p$, and RoCoV all lie in the H area related to their membership functions. In addition, the assessment is related to Segment 2, and the H_2 membership function corresponds to the time. However, the previous voltage magnitude sample is located in a safe area. The input variables relevant to the $RoCoV$ behavior refer to the method of the voltage trend to the high-voltage condition. This is interpreted as an emergency situation.

The third row of Table I shows that the voltage magnitude slope, $RoCoV_p$, and RoCoV are located in a safe area. Based

on this combination, the voltage magnitude lies between 0.95 and 1.05 p.u. in the L_2 membership function of time in Segment 2. In addition, the previous voltage magnitude sample is less than 0.8 p.u., whereas the voltage trend is desirable. This results in an alarm status in the output of the fuzzy-logic method due to the history of the voltage. The fourth combination as listed in Table I refers to the normal status derived from the reliable voltage trajectory at this instant.

Another combination is shown in the fifth row of Table I, where the voltage magnitude is less than 0.95 p.u., the time evaluation belongs to the second part of Segment 3, and $RoCoV_p$ is less than that of previous sample with a negative value. In addition, the first voltage magnitude is between 0.8 and 0.95 p.u.. Thus, the voltage trajectory follows a worse direction than before, indicating a high-risk state. This state highlights an undesirable condition and raises the weighting factor of this moment compared with previously reported results in the averaging procedure. More precisely, the voltage, located between 0.9 and 0.95 p.u. in the second part of Segment 3 with the undesirable trend, is classified similarly to a state in which the voltage is outside the predefined area. This state is highlighted after averaging process with the previous ones. This state may result in low-cost and small preemptive actions, including small blocks of load shedding, to return the voltage trend into the secure area.

The combination of arrays in the sixth row in Table I must be considered. The voltage trajectory is evaluated in the second part of Segment 2, which is less than 0.8 p.u. with respect to array (6, 8) in Table I. We can conclude that the voltage trend is worse than that of the previous sample based on array (6, 5) and array (6, 6). In addition, array (6, 7) shows that the previous voltage magnitude is less than 0.8 p.u.. Thus, this condition causes the fuzzy logic to assign this moment into a high-risk situation.

If the voltage trajectory exits a predefined framework, it is considered a high-risk situation that may lead to generator disconnection and increase the risk of voltage instability. Investigating the voltage behavior within a predefined framework provides useful information about the transient voltage trend and the capacity of the power system to meet the load requirements after fault clearance. The proposed method considers the generator voltage, indirectly indicating the load bus voltage status for voltage assessment. In some cases, the generator voltage may remain within the predefined area, whereas the load bus voltage may lead to instability, affecting the generator voltage with a time delay. Therefore, detailed information about the generator voltage is essential to predict the future trends of the system and help SOs implement cost-effective measures to maintain system stability.

The most common countermeasures against the undesired voltage profile can range from capacitor banks and flexible alternating current transmission systems to shedding small blocks of loads. The Mamdani method, as a fuzzy inference method, is used for the fuzzy-logic method, and defuzzification is performed using the centroid method.

Following fuzzy-logic decision making, an averaging process is performed on the output variable in a moving window consisting of five samples, as expressed in (8).

$$S_{up}=\begin{cases}\sum_{1}^{j}\dfrac{Out_j}{j} & j<5\\ \sum_{j-5}^{j}\dfrac{Out_j}{5} & j\geq 5\end{cases} \tag{8}$$

where Out_j is the output of the j^{th} sample.

This process provides more reliable results based on the voltage conditions. Considering four prior samples with identical weighting coefficients prevents unnecessary decision making and provides comprehensive results. This process results in the decisions that lead to conservative and reliable preemptive actions against the undesired voltage profile.

IV. Simulation Results and Discussion

A. Benchmark System

Different contingencies are applied to a IEEE 73-bus power system to investigate the performance of the proposed method in terms of voltage-status classification. The case study consists of 33 generating units distributed across three areas. Figure 12 shows a single-line diagram of the IEEE 73-bus power system. Bus 223 is selected as the pilot bus in this paper.

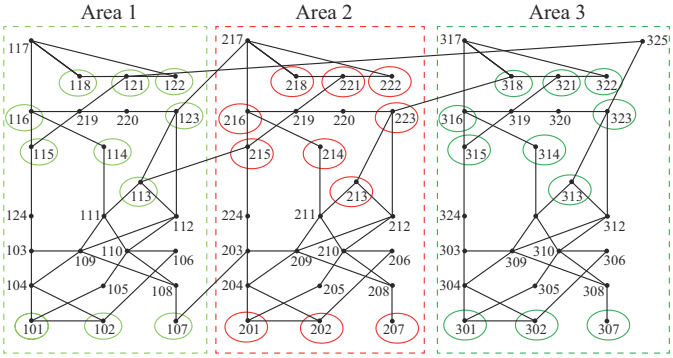

Fig. 12. Single-line diagram of IEEE 73-bus power system.

B. Simulation Results

A three-phase fault with $R=0.001\ \Omega$ is applied to Line 208-210 at $t=0.5$ s and lasts for 0.35 s. The fault point distance from bus 208 is 20% of the line length. The proposed method determines the voltage status of bus 207, as shown in Fig. 13. Note that the blue cross in the figures denotes instantaneous fuzzy logic output.

The voltage magnitude trajectory of bus 207 approaches an unstable state after fault clearance. Thus, the voltage classification results indicate a high-risk situation. It can be observed from Fig. 13 that the voltage magnitude is in an emergency status early in the Segment 1 area and then tends to be uncontrolled.

By contrast, the proposed method analyzes the voltage magnitude status of bus 202 following a three-phase fault on Line 208-209. The symmetrical fault occurrence with $R=0.001\ \Omega$ remains on the line for 0.3 s from $t=0.5$ s at a distance from bus 208 for half of the line length.

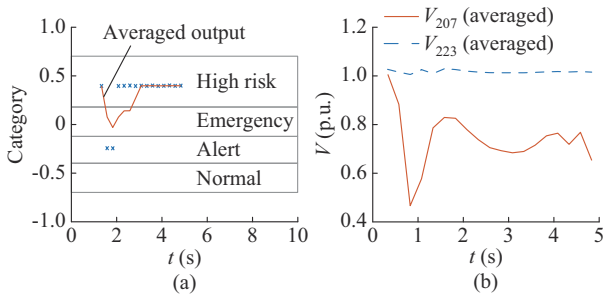

Fig. 13. Assessment results after a three-phase fault with $R=0.001$ Ω on Line 208-210 for 0.35 s. (a) Averaged and instantaneous outputs of fuzzy-logic controller. (b) Averaged voltage magnitudes of pilot bus 223 and bus 207.

The averaged voltage magnitude trajectory exceeds the upper bound in Segment 1 at a specified time and returns to acceptable conditions. In addition, the voltage trajectory in Segment 2 follows an incremental trend for a limited duration. Accordingly, this condition is dedicated to alarm situations under the proposed classification. The voltage then follows a smooth trajectory in a secure form. Figure 14 shows the assessment results after a three-phase fault with $R=0.001$ Ω on Line 208-209 for 0.3 s.

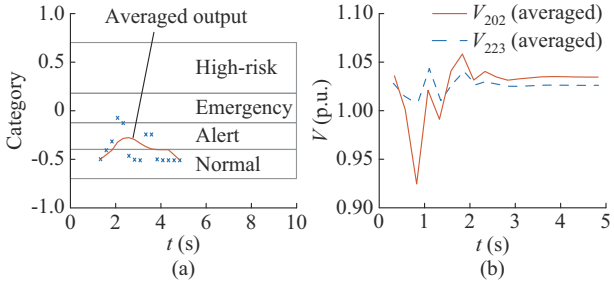

Fig. 14. Assessment results after a three-phase fault with $R=0.001$ Ω on Line 208-209 for 0.3 s. (a) Averaged and instantaneous outputs of fuzzy-logic controller. (b) Averaged voltage magnitudes of pilot bus 223 and bus 202.

Another three-phase fault with $R=0.1$ Ω from $t=0.5$ s to $t=0.8$ s on Line 219-220 exposes the stability of the power system under a threat. The fault occurrence is imposed on the middle line. The average voltage of bus 216, as shown in Fig. 15, experiences low-frequency oscillations. Based on the proposed principle of voltage classification, the voltage magnitudes in Segments 2 and 3 follow an undesirable trajectory, leading to unstable circumstances.

However, in these cases, the voltage trajectory may instantaneously cross safe conditions, approaching an undesired boundary, as shown in Fig. 15. Although the fuzzy-logic block issues a flag of normal status at this instant, the averaged output considers the background of the voltage trajectory. Thus, the effect of this instant is alleviated in decision making.

At this stage, a three-phase fault with $R=0.001$ Ω on Line 216-219 from $t=0.5$ s to $t=0.8$ s challenges the proposed classification performance. The fault point distance from bus 216 is 20% of the line length. The results show that the voltage magnitude experiences severe oscillations because of the unstable power swing following the fault occurrence, as shown in Fig. 16(c). Thus, the averaged voltage magnitude of the phasor measurement unit (PMU) data follows a low voltage trajectory, which results in a high-risk situation. Therefore, the output of the proposed method confirms the undesirable voltage conditions. Figure 16 shows the assessment results after a three-phase fault with $R=0.001$ Ω on Line 216-219 from $t=0.5$ s to $t=0.8$ s.

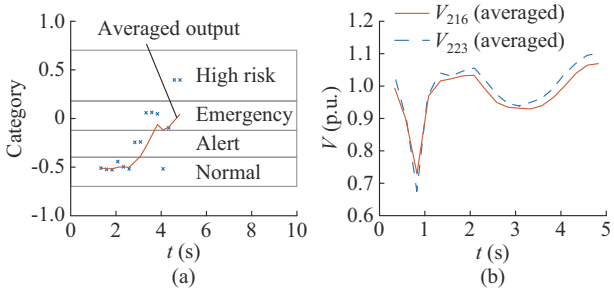

Fig. 15. Assessment results after a three-phase fault with $R=0.1$ Ω on Line 219-220 from $t=0.5$ s to $t=0.8$ s. (a) Averaged and instantaneous outputs of fuzzy-logic controller. (b) Averaged voltage magnitudes of pilot bus 223 and bus 216.

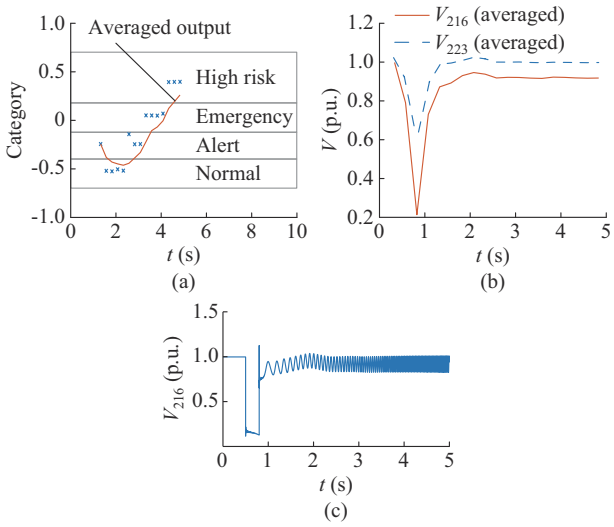

Fig. 16. Assessment results after a three-phase fault with $R=0.001$ Ω on Line 216-219 from $t=0.5$ s to $t=0.8$ s. (a) Averaged and instantaneous outputs of fuzzy-logic controller. (b) Averaged voltage magnitudes of pilot bus 223 and bus 216. (c) Instantaneous voltage trajectory of bus 216.

In addition, the voltage trajectory of bus 216 following a three-phase fault with $R=0.001$ Ω on Line 222-217 is categorized based on the proposed method, as shown in Fig. 17. The fault point distance from bus 222 is 90% of the line length.

The voltage profile after the fault clearance at $t=0.8$ s as shown in Fig. 17 reveals that the voltage follows an undesirable trend in Segment 3. Accordingly, the voltage status derives from a process that approaches a high-risk situation. In this case, the voltage decreases for several sequential samples, indicating a low-voltage threat.

C. Comparison and Discussion

For voltage assessment, the performance of the proposed method is compared with several popular indices, including TVSI, VSRI, TVI, contingency severity index (CSI), and estimated time for voltage recovery (denoted as TR).

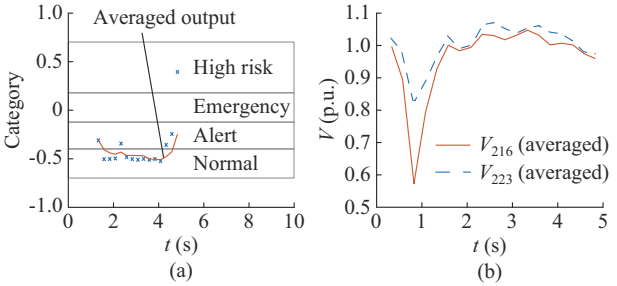

Fig. 17. Assessment results after a three-phase fault with $R=0.001$ Ω on Line 222-217 from $t=0.5$ s to $t=0.8$ s. (a) Averaged and instantaneous outputs of fuzzy-logic controller. (b) Averaged voltage magnitudes of pilot bus 223 and bus 216.

The characteristics of these indices are briefly introduced as follows. Additional details can be found in [14] and [19].

TVSI indicates the instances in which the difference between the initial and current values of the voltage profile exceeds a specific threshold. The sum of these differences determines the voltage status after fault clearance up to the time of the STVS evaluation.

VSRI determines the voltage status based on the voltage behavior in a window with a length of several samples. The average voltage value obtained using a moving window is then compared with the most recent voltage sample.

TVI determines the sum of the areas in which the voltage trajectory exceeds the exponential upper and lower boundaries.

CSI uses two indices to obtain the VS status. The first index is related to the duration in which the voltage trajectory remains below a specific value, and the second index indicates the minimum value of the voltage after fault clearance.

Finally, serving as an indicator of load shedding, TR is introduced in the paper. This index is derived from the voltage deviation and estimated time required for voltage restoration to a safe level. Specifically, the index quantifies the time necessary for voltage recovery when the voltage remains less than 0.8 p.u. after fault clearance. If the estimated time exceeds the prespecified time for restoration, load shedding is automatically initiated. The estimated time is determined by the slope of the voltage trajectory, where a negative slope indicates an infinite recovery time and a positive slope allows for an estimation of the recovery time. One can obtain the estimated recovery time, which is calculated as follows.

$$T_{es}(t_k)=\begin{cases}\dfrac{0.8-V(t_k)}{V(t_k)-V(t_k-\Delta t)}\Delta t & \dfrac{V(t_k)-V(t_k-\Delta t)}{\Delta t}>0\\ infinite & \dfrac{V(t_k)-V(t_k-\Delta t)}{\Delta t}\le 0\end{cases} \tag{9}$$

where T_{es} is the estimated time; t_k is the current sample after the fault occurrence; and $V(t_k)$ is the voltage magnitude at the k^{th} sample of the time. T_{es} is then compared with the predetermined time T_{req} for recovery after fault clearance as follows.

$$T_r(t_k)=(t_k+T_{es}(t_k))-(t_c+T_{req}) \tag{10}$$

where t_c and T_r are the clearance time and time index, respectively. The triggering of load shedding depends on the estimated time being greater than zero, which is necessary to restore the voltage to a secure level.

In this regard, two scenarios are considered to compare the proposed and previous methods.

1) The system operates at 120% of a base load. Then, a three-phase fault with a resistance of 0.001 Ω is applied to Line 216-219. The fault point distance from bus 216 is 20% of the line length that lasts for 0.3 s from $t=0.5$ s.

2) The power system operates at 110% of the base load. Then, a three-phase fault is applied to Line 216-219 with a property similar to that of Scenario 1.

Figure 18 shows the voltage magnitudes of bus 216 in response to Scenarios 1 and 2. The results of the proposed method and aforementioned indices in response to Scenario 1 are presented in Fig. 19.

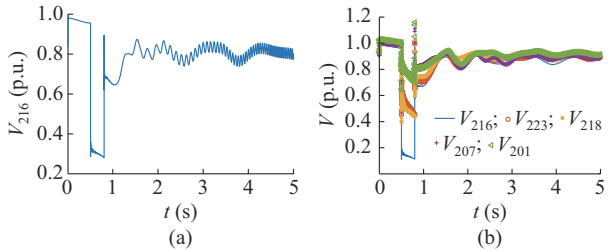

Fig. 18. Voltage magnitudes of bus 216 in response to Scenarios 1 and 2. (a) Scenario 1. (b) Scenario 2.

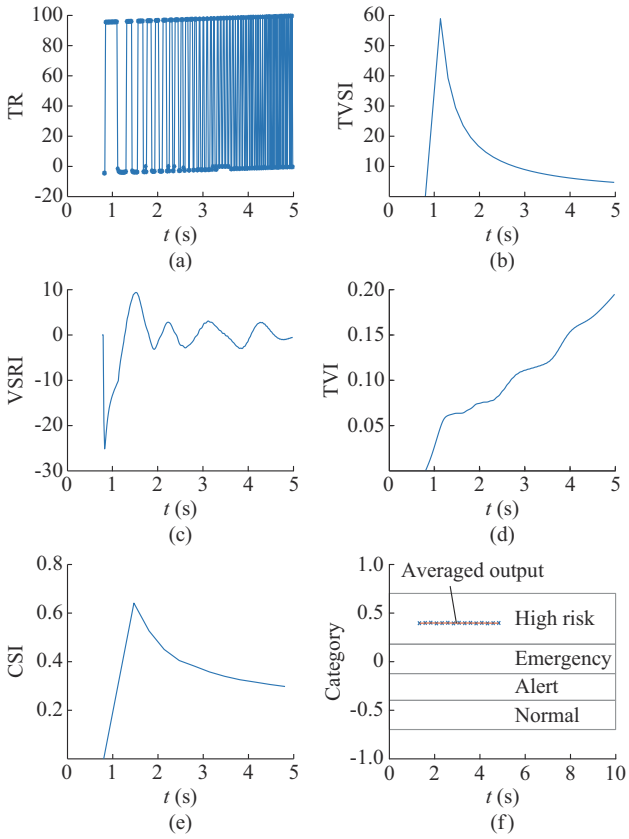

Fig. 19. Results in response to Scenario 1. (a) TR profile after applying scenario. (b) TVSI profile for different time intervals. (c) VSRI profile in response to applied scenario over time. (d) TVI profile. (e) CSI profile for different time intervals. (f) Results with proposed method.

Figure 19(a) presents the differences between the estimated and predetermined time for voltage recovery at each instance. For clarity, the values associated with infinite estimated time and when the voltage is greater than 0.8 p.u. are assumed to be 10 and 0, respectively. Figure 19(a) shows that the time index frequently changes between negative values with safe trends and infinite values under unsafe conditions. This behavior occurs because of the oscillatory trend of the voltage even when it is less than 0.8 p.u.. The duration time for slope calculation is a critical factor in making appropriate decisions. However, the index may face challenges in making appropriate decisions in oscillatory voltage situations and in obtaining an index value based on previous voltage samples.

In addition, the index is useful only under conditions in which the voltage remains less than 0.8 p.u. for 4 s after a fault occurrence. Finally, the index does not provide classification information about the voltage trajectory when it is greater than 0.8 p.u. under this time duration.

TVSI results, as shown in Fig. 19(b), reveal that the TVSI is adversely affected by the time interval used in VS assessment. Determining a suitable threshold for TVSI requires further study as this index depends on different time intervals and benchmarks.

In addition, TVSI uses local indices from other locations to generate a global index and therefore cannot be used as a local indicator of VS.

Figure 19(c) shows the VSRI trajectory, which measures the voltage differences with their historical trends in a moving window and presents a global index for the considered buses. With respect to the VSRI concept, the index values follow a trend of approximately 0 when the voltage tracks a small oscillation direction. Thus, despite the low oscillation of the index in this scenario, the voltage profile shown in Fig. 18 exhibits unacceptable behavior. In addition, determining the VSRI threshold makes it difficult to represent the voltage status of the power system based on the benchmark and requires studies at different time intervals. Another challenge is that the number of required samples involved in the moving window changes the value of the index, making the process for determining the threshold definition more difficult.

TVI is an index that determines whether the voltage can remain in a predefined area, indicating the time duration at which the voltage surpasses the lower or upper bound. According to Fig. 19(d), the TVI value increases over time after fault clearance, indicating a condition in which the voltage remains outside the predefined area. Another challenge is determining parameters B and v_{st}, which are involved in the formulation of the upper and lower bounds, as shown in (11). This determination does not follow a specific process and requires greater accuracy. When the focus is on the earlier evaluation time after fault clearance, the values of the parameters are defined such that the index fails to capture the appropriate properties for a long period, and vice versa.

$$T_{low}(t)=\frac{\left(\frac{t}{t_f}\mathrm{e}^{\frac{1}{t_f}}\right)^B}{\mathrm{e}^B}v_{st} \tag{11}$$

where $T_{low}(t)$ is the lower exponential border for the voltage; v_{st} is the steady-state voltage; B is the damping factor; and t_f is the end of the evaluation time.

Figure 19(e) illustrates the response of the CSI, which considers the time intervals during which the voltage drops to a predetermined threshold. As shown in the CSI trajectory in Fig. 19(e), the index presents significant values for short durations while converging toward lower values for longer periods. Similar to previous indices, the CSI has difficulty in determining the appropriate thresholds for voltage assessment across different time intervals.

The proposed method is then employed to showcase the response to Scenario 1, as depicted in Fig. 19(f). The results demonstrate that the proposed method offers a reliable assessment of the VS and effectively identifies unacceptable voltage behaviors without relying on predefined thresholds. This capability enables the implementation of effective countermeasures to prevent uncontrolled situations.

Figure 20 shows the responses of the evaluated indices, including TR, TVSI, VSRI, TVI, CSI, and the proposed method, to Scenario 2 for performance evaluation.

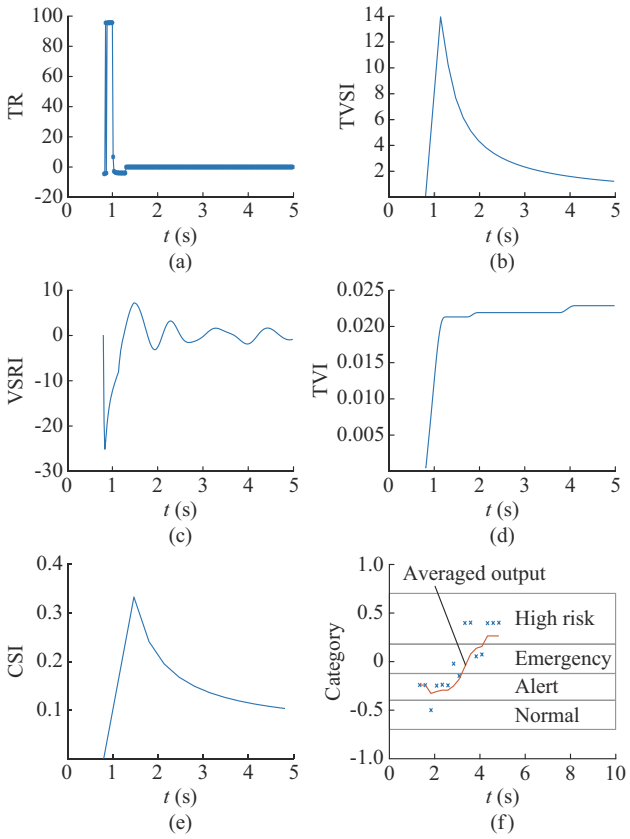

Fig. 20. Responses of evaluated indices to Scenario 2. (a) TR profile after applying scenario. (b) TVSI profile for different time intervals. (c) VSRI profile in response to applied scenario over time. (d) TVI profile. (e) CSI profile for different time intervals. (f) Results with proposed method.

Table II presents the results obtained using the considered indices and proposed method in response to Scenario 2, as depicted in Fig. 20. Table III details the properties and features of the proposed method in comparison with the existing predictive methods and popular indices used in assessing

the voltage status throughout the evaluation period.

TABLE II
COMPARISON OF SELECTED INDICES AND PROPOSED METHOD IN RESPONSE TO SCENARIO 2

Index	Comparison
Voltage trajectories	Voltage trajectories are stable after the fault clearance but follow a risky trend requiring suitable corrective measures to return the voltage to a safe bound.
TVSI	TVSI is damped over time following a considerable increase after t_{cl}. In this case, it does not present clear information, particularly for a long time.
VSRI	It oscillates around zero with low magnitudes. It does not present an accurate assessment while the voltage follows a risky trend.
CSI	Although the voltage tracks a vulnerable trend in the long time interval, the CSI has low values and does not provide accurate information.
TVI	It has low values over time after the fault clearance while the voltage remains below 0.95 p.u. for a long time, indicating a potential risk.
TR	The output of this index at initial time results in load shedding, which may not be necessary for early stages of this scenario with respect to the voltage trend.
Proposed method	The proposed method classifies the applied disturbance to prepare for potential corrective action at low costs.

To clarify the statistics of the applied disturbances in evaluating the performance of the proposed method, we must refer to the 53 states that indicate successful responses to the proposed method.

Table IV presents detailed information about the applied scenarios in the case study to verify the performance of the proposed method.

V. CONCLUSION

Determining of the voltage trend when it lies within a prespecified operation area generates more precise situational awareness and prevents undesirable conditions. Accordingly, the proposed method focuses on this issue and provides a classification method for the generating-side voltage trajectories following severe disturbances. An adaptive fuzzy-logic method is introduced to categorize the voltage status by considering FIDVR, STVI, and oscillation effects. In the proposed method, a fuzzy-logic controller consisting of eight MFs conducts the intended classification. In addition, the membership function parameters are adaptively determined over time.

Simulations are conducted using an IEEE 73-bus power system to confirm the effectiveness of the proposed method.

Accordingly, the proposed method presents a solution that has the following features.

1) The classification method provides more opportunities for operators to take countermeasures against undesirable conditions.

2) The proposed method considers different variables to participate in decision making and to generate comprehensive results.

3) The adaptive process of membership function determination enables the proposed method to be more flexible under current conditions.

TABLE III
COMPARISONS OF PROPERTIES OF PREDICTIVE-BASED METHOD, SELECTED INDICES, AND PROPOSED METHOD

Index	Comparison
Predictive-based methods	They need Thevenin equivalent circuit parameters at each load bus and components model as a challenge, especially for emerging time-varying flexible loads. Generally, predictive methods can be only used for long-term stability assessment.
TVSI	It needs a proper threshold to provide an accurate assessment. It does not present detailed information when the voltage stays in predefined area. The criterion for index calculation changes from one case to another.
VSRI	It compares the voltage with its past behavior in a specific moving window. The window length determination for averaging is challenging. It needs a proper threshold to assess the voltage assessment. It needs the local information from other locations. If the voltage follows a smooth trend but outside the safe area, it cannot provide an accurate decision.
CSI	CSI cannot determine voltage risky status when it is higher than 0.8 times of pre-disturbance voltage, especially in long time. It needs for load bus information to provide better decisions. It needs to determine a proper threshold for different time intervals.
TVI	Parameter definition to specify safe area is challenging to provide a proper trade-off between short- and long-time assessment. It needs to determine a proper threshold for an accurate assessment. It cannot to provide an awareness when the voltage is higher than 0.9 p.u. but close to it for long time.
TR	Instantaneous values of the voltage are used for decision making. The index performance can be challenging with the border conditions at 0.8 p.u.. During the oscillatory conditions, the risk of the mistakes may increase.
Proposed method	It provides a classification assessment to prepare low-cost corrective actions when the voltage has a potential risk trend. It focuses on generator buses without the need for load buses. It compares the voltage trajectory with the firmest one in that area, unlike the VSRI index. It provides a reliable decision after the specific time interval using averaging the past results in a moving window. Because it considers the behavior voltage inside the predefined area, it needs a proper time interval to provide reliable awarenes for low-cost corrective actions. It needs to wait for 15 new samples for each new decision making result.

TABLE IV
DETAILED INFORMATION OF APPLIED SCENARIOS TO IEEE 73-BUS POWER SYSTEM

Parameter	Value
Loading condition (%) (number of scenarios)	120 (4 scenarios), 115 (7 scenarios), 110 (6 scenarios), 105 (8 scenarios)
Fault resistance (Ω)	0.001, 0.1, 10, 20
Faulted line location	20%, 50%, 80% of line length
Time duration (s)	0.1, 0.2, 0.3, 0.4
Faulted lines	216-219, 219-220, 220-223, 212-223, 213-223, 204-209, 207-208, 202-201, 222-217, 218-217, 318-317, 322-317, 316-319

4) The fuzzy-logic output, after an averaging process, considers the background decisions and provides reliable results.

5) The voltage behavior is compared with the preselected pilot bus voltage, which provides a reliable assessment for decision making.

The proposed method for voltage-stability analysis utilizes data from two PMU locations, eliminating the need for a complex high-bandwidth communication infrastructure. This method streamlines the analytical process and enhances the accuracy and reliability while providing a cost-effective solution.

REFERENCES

[1] N. Hatziargyriou, J. Milanovic, C. Rahmann *et al.*, "Definition and classification of power system stability – revisited & extended," *IEEE Transactions on Power Systems*, vol. 36, no. 4, pp. 3271-3281, Jul. 2021.

[2] C. Andersson, J. E. Solem, and B. Eliasson, "Classification of power system stability using support vector machines," in *Proceedings of 2005 IEEE PES General Meeting*, San Francisco, USA, Jun. 2016, pp. 650-655.

[3] A. Borici, J. L. Rueda Torres, and M. Popov, "Comprehensive review of short-term voltage stability evaluation methods in modern power systems," *Energies*, vol. 14, no. 14, p. 4076, Jul. 2021.

[4] Y. Xu, R. Zhang, J. Zhao *et al.*, "Assessing short-term voltage stability of electric power systems by a hierarchical intelligent system," *IEEE Transactions on Neural Networks Learning System*, vol. 27, no. 8, pp. 1686-1696, Sept. 2015.

[5] H. H. Goh, Q. S. Chua, S. W. Lee *et al*., "Evaluation for voltage stability indices in power system using artificial neural network," *Procedia Engineering*, vol. 118, pp. 1127-1136, Sept. 2015.

[6] B. R. Prusty and D. Jena, "A critical review on probabilistic load flow studies in uncertainty constrained power systems with photovoltaic generation and a new approach," *Renewable and Sustainable Energy Reviews*, vol. 69, pp. 1286-1302, Mar. 2017.

[7] S. You, Y. Zhao, M. Mandich *et al.*, "A review on artificial intelligence for grid stability assessment," in *Proceedings of 2020 IEEE International Conference on Communications, Control, and Computing Technologies for Smart Grids (SmartGridComm)*, Tempe, USA, Nov. 2020, pp. 14-19.

[8] L. Zhu, C. Lu, I. Kamwa *et al*., "Spatial-temporal feature learning in smart grids: a case study on short-term voltage stability assessment," *IEEE Transactions on Industrial Informatics*, vol. 16, no. 3, pp. 1470-1482, Mar. 2020.

[9] O. A. Alimi, K. Ouahada, and A. M. Abu-Mahfouz, "A review of machine learning approaches to power system security and stability," *IEEE Access*, vol. 8, pp. 113512-113531, Jun. 2020.

[10] L. Zhu, C. Lu, and Y. Luo, "Time series data-driven batch assessment of power system short-term voltage security," *IEEE Transactions on Industrial Informatics*, vol. 16, no. 12, pp. 7306-7317, Dec. 2020.

[11] K. Ye, J. Zhao, H. Zhang *et al*., "Data-driven probabilistic voltage risk assessment of miniWECC system with uncertain PVs and wind generations using realistic data," *IEEE Transactions on Power Systems*, vol. 37, no. 5, pp. 4121-4124, Jun. 2022.

[12] Y. Xu, Z. Y. Dong, K. Meng *et al*., "Multi-objective dynamic VAR planning against short-term voltage instability using a decomposition-based evolutionary algorithm," *IEEE Transactions on Power Systems*, vol. 29, no. 6, pp. 2813-2822, Nov. 2014.

[13] S. Wildenhues, J. L. Rueda, and I. Erlich, "Optimal allocation and sizing of dynamic var sources using heuristic optimization," *IEEE Transactiosn on Power Systems*, vol. 30, no. 5, pp. 2538-2546, Oct. 2014.

[14] M. Aslanian, M. E. Hamedani-Golshan, H. H. Alhelou *et al*., "Analyzing six indices for online short-term voltage stability monitoring in power systems," *Applied Science*, vol. 10, no. 12, p. 4200, Jun. 2020.

[15] A. Alshareef, R. Shah, N. Mithulananthan *et al*., "A new global index for short term voltage stability assessment," *IEEE Access*, vol. 9, pp. 36114-36124, Feb. 2021.

[16] M. Glavic, D. Novosel, E. Heredia *et al.*, "Real-time voltage control under stressed conditions, see it fast to keep calm," *IEEE Power Energy Magazine*, vol. 10, pp. 43-53, Jun. 2012.

[17] C. Liu, F. Hu, D. Shi *et al*., "Measurement-based voltage stability assessment considering generator VAR limits," *IEEE Transactions on Smart Grid*, vol. 11, no. 1, pp. 301-311, Jan. 2020.

[18] H. J. Lee, A. K. Srivastava, V. V. G. Krishnan *et al*., "Decentralized voltage stability monitoring and control with distributed computing coordination," *IEEE Systems Journal*, vol. 16, no. 2, pp. 2251-2260, Jun. 2022.

[19] H. Yang, N. Li, Z. Sun *et al.*, "Real-time adaptive UVLS by optimized fuzzy controllers for short-term voltage stability control," *IEEE Transactions on Power Systems*, vol. 37, no. 2, pp. 1449-1460, Mar. 2022.

[20] S. M. Halpin, K. A. Harley, R. A. Jones *et al*., "Slope-permissive under-voltage load shed relay for delayed voltage recovery mitigation," *IEEE Transactions on Power Systems*, vol. 23, no. 3, pp. 1211-1216, Aug. 2008.

[21] North American Electric Reliability Corporation, PRC-024-1. (2021, Jan.). Generator frequency and voltage protective relay settings. [Online]. Available: https://www. nerc. com/pa/Stand/Reliability% 20Standards/PRC-024-2.pdf

[22] Western Electricity Coordination Council, TPL-001-WECC-CRT-3.1. (2016, Aug.). Transient voltage criteria reference document. [Online]. Available: https://www. wecc. org/Reliability/TPL-001-WECC-CRT-3.1. pdf

[23] H. Golpîra, A. Román-Messina, and H. Bevrani, *Renewable Integrated Power System Stability and Control*. New York: John Wiley & Sons, 2021.

Sirwan Shazdeh received the Ph. D. degree in electrical engineering from University of Kurdistan, Sanandaj, Iran, in 2022. Currently, he is an Associate Research Fellow with Smart/Micro Grids Research Center (SMGRC) at the University of Kurdistan. His current research interests include microgrid dynamics and control, smart grid wide-area protection and control.

Hêmin Golpîra received the B. Sc., M. Sc., and Ph. D. degrees (with Hons.) in electrical engineering in 2007, 2009, and 2015, respectively. During 2014-2015, he was an Associate Fellow with the University of Wisconsin-Madison, Madison, USA. In 2016, he joined the University of Kurdistan, Sanandaj, Iran, where he is currently an Associate Professor. His research interests include power system dynamics and stability, renewable energy integration, power system modeling and simulation, and wide-area monitoring and control.

Hassan Bevrani received the Ph. D. degree in electrical engineering from Osaka University, Osaka, Japan, in 2004. Currently, he is an IEEE Fellow, and a Professor and the Program Leader of Smart/Micro Grids Research Center (SMGRC) at the University of Kurdistan, Sanandaj, Iran. Over the years, he has worked as Senior Research Fellow and Visiting Professor with Osaka University, Kumamoto University, Kumamoto, Japan, Kyushu Institute of Technology, Kyushu, Japan, Doshisha University, Kyoto, Japan, Nagoya University, Nagoya, Japan, Queensland University of Technology, Brisbane, Australia, Ecole Centrale de Lille, Lille, France, and Technical University of Berlin, Berlin, Germany. His current research interests include microgrid dynamics and control, smart grid operation and control, and intelligent/robust control applications in power electric industry.